





Article

Manganobadalovite, $\text{NaNaMn}(\text{MgFe}^{3+})(\text{AsO}_4)_3$, a New Alluaudite-Group Mineral from the Tolbachik Volcano, Kamchatka, Russia

Natalia N. Koshlyakova ^{1,*}, Igor V. Pekov ¹, Dmitry I. Belakovskiy ², Marina F. Vigasina ¹, Natalia V. Zubkova ¹, Atali A. Agakhanov ², Sergey N. Britvin ³, Anna G. Turchkova ¹, Elena S. Zhitova ⁴, Evgeny G. Sidorov ^{4,†} and Dmitry Yu. Pushcharovsky ¹

¹ Faculty of Geology, Lomonosov Moscow State University, Vorobievsky Gory, 119991 Moscow, Russia; igorpekov@mail.ru (I.V.P.); vigasina@geol.msu.ru (M.F.V.); n.v.zubkova@gmail.com (N.V.Z.); annaturchkova@mail.ru (A.G.T.); dmitp@geol.msu.ru (D.Y.P.)

² Fersman Mineralogical Museum of the Russian Academy of Sciences, Leninsky Prospekt 18-2, 119071 Moscow, Russia; dmzvr@mail.ru (D.I.B.); atali99@mail.ru (A.A.A.)

³ Department of Crystallography, St. Petersburg State University, University Embankment 7/9, 199034 St. Petersburg, Russia; sbritvin@gmail.com

⁴ Institute of Volcanology and Seismology, Far Eastern Branch of Russian Academy of Sciences, Piip Boulevard 9, 683006 Petropavlovsk-Kamchatsky, Russia; zhitova_es@mail.ru (E.S.Z.)

* Correspondence: nkoshlyakova@gmail.com

† Deceased 20 March 2021.

Abstract

The new alluaudite-group mineral manganobadalovite (IMA 2020-035), ideally $\text{NaNaMn}(\text{MgFe}^{3+})(\text{AsO}_4)_3$, was found in the Arsenatnaya fumarole, the Second scoria cone of the Northern Breakthrough of the Great Tolbachik Fissure Eruption 1975–1976, Tolbachik volcano, Kamchatka peninsula, Far-Eastern Region, Russia. Manganobadalovite is a fumarolic mineral, and its aggregates are found overgrowing basalt scoria or exhalative hematite crystal crusts. Associated minerals are badalovite, hematite, cassiterite, sanidine, glauberite and metathénardite. Manganobadalovite occurs as prismatic to equant crystals up to 0.8 mm long typically combined in open-work clusters; it also forms grains that are irregular in shape and cavernous granular crusts up to 0.5 cm. The mineral is transparent, with vitreous luster, and its color varies from red to yellow. Manganobadalovite is brittle and has a noticeable cleavage in one direction and uneven fracture. The calculated density is 4.108 g cm^{-3} . Manganobadalovite is optically biaxial (+), $\alpha = 1.790$ (7), $\beta = 1.800$ (7), $\gamma = 1.815$ (8) and $2V_{\text{meas}} = 80$ (5)°. Chemical composition (wt.%, electron-microprobe): Na_2O 8.75, K_2O 0.17, MgO 5.32, CaO 3.68, MnO 10.09, CuO 0.42, Al_2O_3 0.18, Fe_2O_3 13.90, V_2O_5 0.42, As_2O_5 56.75, total 99.68. The empirical formula calculated based on 12 O apfu is $\text{Na}_{1.69}\text{K}_{0.02}\text{Ca}_{0.39}\text{Mn}_{0.85}\text{Mg}_{0.79}\text{Cu}_{0.03}\text{Fe}^{3+}_{1.04}\text{Al}_{0.02}(\text{As}_{2.96}\text{V}_{0.03})\Sigma_{2.99}\text{O}_{12}$. The crystal structure was solved using single-crystal XRD data, $R = 2.30\%$. Manganobadalovite is monoclinic, $C2/c$, $a = 12.1848(5)$, $b = 12.8924(4)$, $c = 6.6970(3)$ Å, $\beta = 113.113(5)^\circ$, $V = 967.60(7)$ Å³ and $Z = 4$. The strongest reflections of the powder XRD pattern are $[d, \text{Å}(I)(hkl)]$: 6.43(30)020, 3.589(32)(−131, 310), 3.215(38)(040, −112), 3.079(23)(221, 002), 2.941(32)(−312, −222, −331), 2.852(15)(041), 2.788(100)(330, 400, 240, 022), 2.649(22)(−402, 112), 2.626(25)(−132). Manganobadalovite is named as an analogue of badalovite $\text{NaNaMg}(\text{MgFe}^{3+})(\text{AsO}_4)_3$ with Mn^{2+} prevailing in the $M(1)$ site.

Keywords: manganobadalovite; new mineral; alluaudite group; arsenate; crystal structure; fumarole sublimate; Tolbachik volcano; Kamchatka



Academic Editors: Sytle M. Antao and Juan Gómez-Barreiro

Received: 18 December 2025

Revised: 25 January 2026

Accepted: 26 January 2026

Published: 28 January 2026

Copyright: © 2026 by the authors.

Licensee MDPI, Basel, Switzerland.

This article is an open access article distributed under the terms and

conditions of the [Creative Commons Attribution \(CC BY\) license](https://creativecommons.org/licenses/by/4.0/).

1. Introduction

Manganobadalovite $\text{NaNaMn}(\text{MgFe}^{3+})(\text{AsO}_4)_3$ is a new alluaudite-group arsenate found in exhalations of the Arsenatnaya fumarole located at the apical part of the Second scoria cone of the Northern Breakthrough of the Great Tolbachik Fissure Eruption 1975–1976, Tolbachik volcano, Kamchatka peninsula, Far-Eastern Region, Russia ($55^\circ 41' \text{ N}$, $160^\circ 14' \text{ E}$, 1200 m asl) [1].

Arsenatnaya is an active, high-temperature, oxidizing type fumarole, with unique and extremely rich exhalative mineral assemblages. More than 210 (!) mineral species have been identified here, and for 73 of them Arsenatnaya is the type locality. The name to the Arsenatnaya fumarole was given due to the abundance in the exhalations of diverse anhydrous high-temperature arsenates, among which the alluaudite-group minerals are particularly notable for their abundance and chemical variability. Therefore, the Arsenatnaya fumarole offers an exceptional opportunity to study the crystal chemistry of this mineral group. Fourteen out of the sixteen anhydrous arsenates of the alluaudite group (except arseniopleite and caryinite) occur in the volcanic exhalations here, and the majority of them were first discovered in Arsenatnaya and remain endemic to the locality. The first discovered alluaudite-group arsenates are as follows: leybovite-K [2], magnesiohatertite [3], manganohaterite [4], calciohatertite [5], paraberzeliite [6], khrenovite [7], calciojohillerite [8], badalovite [9] and manganobadalovite. In addition, in the samples from the locality the existence of extensive solid solutions between all present alluaudite-type arsenates was verified [10]. For the alluaudite-type mineral johillerite, one of the most abundant arsenates in the fumarole, the crystal chemistry and chemistry of solid solutions were studied in detail [11].

A description of Arsenatnaya and its mineralization is given in [10,12,13], and an overview of the unique fumarolic systems of the Tolbachik volcano, including the list of all new Tolbachik minerals discovered prior to 2020, is given in [14].

Manganobadalovite is named according to the current alluaudite group nomenclature [15] as an analogue of badalovite $\text{NaNaMg}(\text{MgFe}^{3+})(\text{AsO}_4)_3$, with Mn^{2+} prevailing in the octahedral $M(1)$ site. The new mineral and its name have been approved by the IMA Commission on New Minerals, Nomenclature and Classification, IMA2020–035. The IMA-accepted symbol is Mbdl. The type specimen is deposited in the systematic collection of the Fersman Mineralogical Museum of the Russian Academy of Sciences, Moscow, with the catalogue number 97014.

2. Methods

The Raman spectrum of manganobadalovite was obtained on a randomly oriented crystal using an EnSpectr R532 instrument (Chernogolovka, Russia) at the Department of Mineralogy, Lomonosov Moscow State University with a green laser (532 nm) at room temperature. The output power of the laser beam was about 14 mW. The spectrum was processed using the EnSpectr expert mode program in the range from 100 to 4000 cm^{-1} with the use of a holographic diffraction grating with $1800 \text{ lines mm}^{-1}$ and a resolution of 6 cm^{-1} . The diameter of the laser spot on the sample was about $5 \mu\text{m}$. The backscattered Raman signal was collected with a $40\times$ objective; the acquisition time for a single scan was 1000 ms; and the signal was averaged over 100 scans. The mineral is stable under a laser beam.

The determination of the chemical composition of manganobadalovite (Table 1) was carried out in the Laboratory of Analytical Techniques of High Spatial Resolution, Dept. of Petrology, Moscow State University, using a JEOL JXA 8230 Superprobe instrument (Jeol, Japan). Electron microprobe analyses (EMPAs) were carried out in WDS mode (20 kV and 20 nA; the beam diameter is $3 \mu\text{m}$). The reference materials

used are as follows: jadeite (Na, Al), KTiOPO_4 (K), CaSiO_3 (Ca), olivine (Mg), MnTiO_3 (Mn), Cu (Cu), FeS_2 (Fe), V (V) and GaAs (As). The contents of other elements with atomic numbers higher than carbon are below detection limits.

Table 1. Averaged chemical composition of manganobadalovite holotype sample.

Constituent	Wt. %	Range	Stand. Dev.	Probe Standard
Na_2O	8.75	8.60–8.89	0.15	jadeite
K_2O	0.17	0.16–0.19	0.01	KTiOPO_4
MgO	5.32	4.72–5.95	0.51	Olivine
CaO	3.68	3.21–3.87	0.31	CaSiO_3
MnO^1	10.09	9.82–10.57	0.33	MnTiO_3
CuO	0.42	0.35–0.44	0.05	Cu
Al_2O_3	0.18	0.09–0.27	0.09	Jadeite
Fe_2O_3^1	13.9	13.83–13.95	0.05	FeS_2
V_2O_5	0.42	0.27–0.69	0.13	V
As_2O_5	56.75	56.23–57.62	0.63	GaAs
Total	99.68			

¹ Fe is considered as Fe^{3+} and Mn as Mn^{2+} based on the crystal structure data (see below).

The powder X-ray diffraction (XRD) study of manganobadalovite was performed at the Center for X-Ray Diffraction Research of the Science Park of St. Petersburg State University. Diffraction data (Table 2) were collected with a Rigaku R-AXIS Rapid II diffractometer (Rigaku Corporation, Tokyo, Japan) equipped with a cylindrical image plate detector using Debye–Scherrer geometry and $\text{CoK}\alpha$ radiation, at an accelerating voltage of 40 kV, current of 15 mA and exposure time of 15 min. The distance between the sample and the detector was 127.4 mm. The data were integrated using the software package Osc2Tab [16].

Table 2. Powder X-ray diffraction data (d in Å) of manganobadalovite.

I_{obs}	d_{obs}	I_{calc}^1	d_{calc}^2	hkl
2	8.42	1	8.46	110
30	6.43	34	6.45	020
1	5.86	1	5.88	−111
15	5.58	22	5.60	200
3	4.446	2	4.453	021
7	4.395	6	4.398	111
12	4.216	14	4.229	220
10	4.089	10	4.099	−221
1	4.005	2	4.013	130
11	3.766	12	3.782	−311
32	3.589	24, 21	3.602, 3.588	−131, 310
2	3.295	2	3.301	−202
38	3.215	6, 50	3.223, 3.216	040, −112
6	3.160	7	3.165	131
23	3.079	10, 14	3.086, 3.080	221, 002
32	2.941	33, 14, 2	2.951, 2.938, 2.911	−312, −222, −331
15	2.852	20	2.856	041
100	2.788	10, 47, 100, 10	2.819, 2.802, 2.794, 2.779	330, 400, 240, 022
6	2.739	6	2.749	−421
22	2.649	13, 22	2.655, 2.652	−402, 112
25	2.626	38	2.628	−132
6	2.561	8	2.570	420
3	2.448	5	2.455	−422

Table 2. Cont.

I_{obs}	d_{obs}	I_{calc}^1	d_{calc}^2	hkl
2	2.338	3	2.339	202
3	2.308	3, 3	2.317, 2.306	331, −242
3	2.294	2	2.292	132
9	2.201	9	2.208	510
2	2.165	2	2.169	−313
9	2.116	7, 3	2.122, 2.119	350, −531
1	2.062	2	2.049	−442
5	2.034	4, 2	2.037, 2.029	−152, 061
8	2.016	14	2.021	−532
6	1.988	3, 3, 4	1.995, 1.991, 1.987	312, −423, 530
12	1.960	12, 2, 1	1.964, 1.959, 1.956	−352, −333, 023
4	1.941	4	1.942	−133
2	1.923	2	1.929	−621
3	1.887	2, 5	1.893, 1.891	242, −622
10	1.867	1, 10	1.872, 1.868	113, 152
12	1.827	6, 15	1.835, 1.827	−243, 332
2	1.799	3	1.801	−262
6	1.771	6, 2	1.774, 1.768	−171, −533
2	1.752	2	1.755	−461
2	1.731	2, 2	1.732, 1.724	133, 531
4	1.709	3, 2, 3, 1	1.714, 1.712, 1.709, 1.707	171, −641, −712, −623
6	1.691	4, 3	1.695, 1.692	422, 550
7	1.683	12, 1	1.686, 1.674	−642, −353
15	1.661	1, 21	1.663, 1.661	−153, −204
13	1.611	17, 2	1.616, 1.612	640, 080
4	1.583	3, 2	1.589, 1.583	710, −514
7	1.571	10, 2	1.574, 1.571	−372, 621
2	1.557	3, 2	1.559, 1.551	081, 461
8	1.541	4, 5, 4	1.543, 1.542, 1.535	442, −281, 512
7	1.529	6	1.530	371
10	1.521	8, 7, 3, 4	1.523, 1.520, 1.519, 1.516	172, −802, 243, −604
6	1.497	2, 5, 1, 2	1.503, 1.500, 1.498, 1.495	−733, 730, 024, −534
11	1.467	12, 4	1.469, 1.465	−444, 281
2	1.430	1, 4	1.435, 1.433	−572, −752
4	1.420	1, 4, 2	1.424, 1.423, 1.421	−481, 570, 190
4	1.411	4	1.412	−373
5	1.406	6, 4	1.406, 1.401	−173, 800
7	1.390	9	1.389	044
2	1.373	2, 1	1.376, 1.375	602, −842
7	1.356	2, 8	1.359, 1.355	−841, 204
3	1.344	2	1.348	731
4	1.334	5	1.336	−573
4	1.325	4, 2, 1	1.326, 1.324, 1.320	552, −843, 173
6	1.314	2, 4	1.316, 1.315	571, −192

¹ For the calculated pattern, only reflections with intensities ≥ 1 are given. ² For the unit-cell parameters obtained from single-crystal data. The strongest reflections are marked with bold type.

Single-crystal X-ray diffraction studies were carried out at the Dept. of Crystallography and Crystal Chemistry, Moscow State University. The data was obtained at room temperature using an Xcalibur S diffractometer equipped with a CCD detector (Oxford Diffraction, Oxford, UK) (for details see Table 3). Data reduction was performed using CrysAlisPro Version 1.171.39.46 [17]. The crystal structure was solved by direct methods and refined with the use of SHELX software package (version 2018/3) [18].

The final R was 2.3% for 1303 unique and observed ($I > 2\sigma(I)$) reflections after merging 7942 measured reflections to 1418 unique reflections with $R_{\text{int}} = 4.21\%$.

Table 3. Crystal data, data collection information and structure refinement details for manganobadalovite.

Formula	$A^{(1)}(\text{Na}_{0.79}\text{Ca}_{0.21})\Sigma 1.00$ $A^{(2)'}(\text{Na}_{0.80}\text{Ca}_{0.05})\Sigma 0.85$ $M^{(1)}(\text{Mn}_{0.55}\text{Ca}_{0.18}\text{Mg}_{0.15}\text{Na}_{0.12})\Sigma 1.00$ $M^{(2)}(\text{Fe}^{3+}_{1.05}\text{Mg}_{0.65}\text{Mn}_{0.30})\Sigma 2.00$ $T(\text{AsO}_4)_3$
Formula weight	598.50
Crystal system, space group, Z	Monoclinic, $C2/c$, 4
a, b, c (Å)	12.1848(5), 12.8924(4), 6.6970(3)
β (°)	113.113(5)
V (Å ³)	967.60(7)
$F(000)$	1123
μ (mm ⁻¹)	13.303
Absorption correction	gaussian
Crystal dimensions (mm)	0.12 × 0.13 × 0.20
Diffractometer	Xcalibur S CCD
Temperature (K)	293
Radiation	MoK α , $\lambda = 0.71073$ Å
θ range (°)	3.160–30.623
Range of h, k, l	−17 → 16, −17 → 18, −9 → 9
No. of measured, independent and observed [$I > 2\sigma(I)$] reflections	7942, 1418, 1303
R_{int}	0.0421
Structure solution	direct methods
Refinement on	F^2
Extinction coefficient	0.00053(9)
$R1$ and $wR2$ for $I > 2\sigma(I)$	0.0230, 0.0457
$R1$ and $wR2$ for all data	0.0277, 0.0475
No. of parameters refined	99
$\Delta\rho_{\text{max}}, \Delta\rho_{\text{min}}$ (e Å ⁻³)	0.649, −0.666
Goof	1.097
Weighting scheme	$w = 1/[\sigma^2(F_o^2) + (0.0144P)^2 + 2.0540P]$ $P = (\text{max of } (0 \text{ or } F_o^2)) + 2F_c^2/3$

3. Results

3.1. Occurrence and General Appearance

The samples with manganobadalovite were collected by us in July 2018 from the deep level of the Arsenatnaya fumarole, about 2.5 m below the earth surface. The temperatures measured using a chromel–alumel thermocouple in this zone during sampling were 350–400 °C.

Aggregates of manganobadalovite overgrow exhalative hematite crystal crusts or directly basalt scoria altered by fumarolic gas. Manganobadalovite occurs as oblique-angled prismatic to equant crystals up to 0.8 mm long and up to 0.5 mm thick typically combined in open-work clusters (Figure 1a) up to 0.5 cm across. Blocky crystals are common. The mineral also forms grains that are irregular in shape and thin, cavernous granular crusts (Figure 1b) up to 3 × 5 mm² in area.

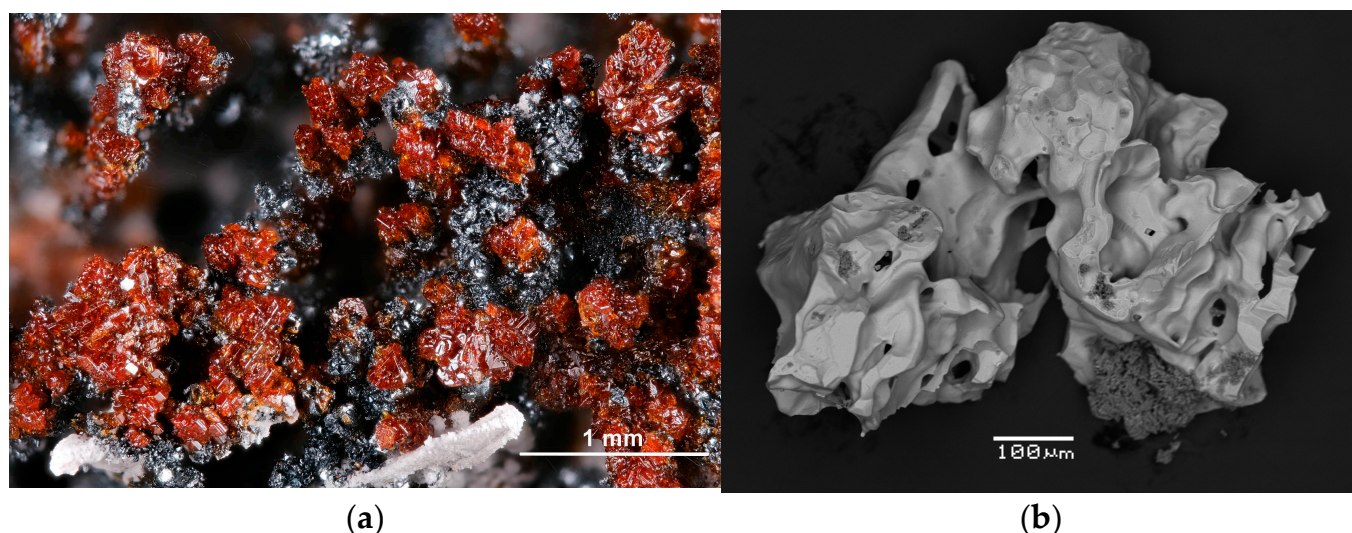


Figure 1. Aggregates of manganobadalovite: (a) clusters of prismatic red crystals up to 0.5 mm in size with white metathénardite on dark steel-grey hematite. Photograph: Maria D. Milshina; (b) fragment of cavernous granular crust, SEM (BSE) image.

Closely associated minerals are badalovite, hematite, cassiterite, sanidine, glauberite and metathénardite.

We believe that manganobadalovite is formed at temperatures not lower than 400–450 °C. It likely formed as a result of the interaction between fumarolic gas and basalt scoria. The latter could be a source of Mg and Ca which have very low volatilities in such post-volcanic systems at temperatures up to 400–500 °C [19].

3.2. Physical Properties and Optical Data

Manganobadalovite ranges in color from red, brownish-red and orange-to-orange-yellow and honey-colored. It is transparent when individual and translucent in aggregates, with a white-to-pale-yellowish streak and vitreous luster. The mineral is brittle, has uneven fracture and a noticeable cleavage in one direction (orientation undetermined). Neither density nor Mohs hardness were measured directly because crystal clusters and granular aggregates are cavernous and typically contain hematite inclusions. The calculated density of the holotype, based on the empirical formula and unit-cell volume obtained from single-crystal X-ray diffraction data, is 4.108 g cm⁻³. The Mohs hardness is presumably about 3, by analogy with other alluaudite-group arsenates.

Manganobadalovite is optically biaxial (+), $\alpha = 1.790$ (7), $\beta = 1.800$ (7), $\gamma = 1.815$ (8) (589 nm); $2V$ (meas.) = 80 (5)° (estimated by the curve of the conoscopic figures on the sections perpendicular to the optical axes), $2V$ (calc.) = 79°. Dispersion of optical axes is noticeable, $r > v$. Like other alluaudite-group arsenates, the optical orientation is assumed to be $Y = b$. In plane-polarized transmitted light, manganobadalovite is reddish-brown and non-pleochroic.

3.3. Raman Spectroscopy

The Raman spectrum of manganobadalovite (Figure 2) was interpreted according to [20]. The strongest bands 859 and 801 cm⁻¹ correspond to stretching vibrations of AsO₄³⁻ distorted tetrahedra. The bands with maxima at 480, 417 and 377 cm⁻¹ correspond to triply degenerate bending vibrations of the same tetrahedra.

The weaker band with maximum at 548 cm⁻¹ can be assigned to Fe³⁺-O stretching vibrations.

The absence of bands with frequencies higher than 950 cm⁻¹ indicates the absence of groups with O-H, C-H, C-O, N-H, N-O and B-O bonds in manganobadalovite.

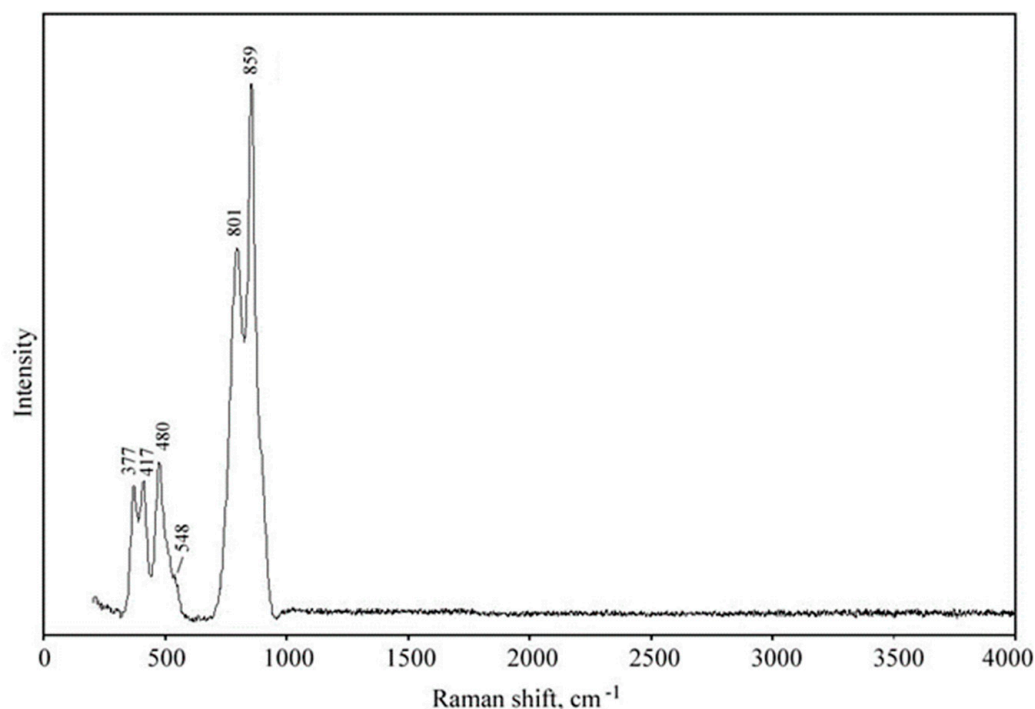


Figure 2. Raman spectrum of manganobadalovite.

3.4. Chemical Composition

The chemical composition of the holotype sample of manganobadalovite, averaged over five spot analyses, is given in Table 1. Fe is considered as Fe^{3+} , and Mn as Mn^{2+} , based on the crystal structure data (see below) and taking into account the strongly oxidizing conditions of mineral formation in the Arsenatnaya fumarole: only Fe^{3+} minerals are found there [10].

The empirical formula calculated on the basis of 12 O atoms per formula unit (*apfu*) is $\text{Na}_{1.69}\text{K}_{0.02}\text{Ca}_{0.39}\text{Mn}_{0.85}\text{Mg}_{0.79}\text{Cu}_{0.03}\text{Fe}^{3+}_{1.04}\text{Al}_{0.02}(\text{As}_{2.96}\text{V}_{0.03})_{\Sigma 2.99}\text{O}_{12}$.

The simplified formula, based on EMPA and crystal structure data is $(\text{Na,Ca},\square)_2(\text{Mn,Ca})(\text{MgFe}^{3+})(\text{AsO}_4)_3$, and the idealized formula is $\text{Na}_2\text{MnMgFe}^{3+}(\text{AsO}_4)_3$ which requires Na_2O 10.37, MgO 6.74, MnO 11.87, Fe_2O_3 13.36, As_2O_5 57.66, total 100 wt.%.

The end-member crystal chemical formula, according to the actual nomenclature of the alluaudite supergroup [15] is $\text{NaNaMn}(\text{MgFe}^{3+})(\text{AsO}_4)_3$.

The correctness of the obtained data is confirmed by the superior value of the Gladstone–Dale compatibility index [21]: $1 - (K_p/K_c) = -0.007$.

3.5. X-Ray Crystallography and Crystal Structure

Powder XRD data of manganobadalovite (for $\text{CoK}\alpha$) are given in Table 2. The unit-cell parameters refined from the powder data are as follows: $a = 12.15$ (2), $b = 12.876$ (9), $c = 6.690$ (9) Å, $\beta = 112.89$ (7)° and $V = 967.60$ (7) Å³.

Crystal data, data collection information and structure refinement details are presented in Table 3. Coordinates and thermal displacement parameters of atoms and bond valence sums are given in Table 4, refined site-scattering factors and assigned occupancies for mixed-occupied cation sites in Table 5 and selected interatomic distances in Table 6.

Table 4. Coordinates and equivalent displacement parameters (U_{eq} , in \AA^2) of atoms and bond-valence sums (BVS) for manganobadalovite.

Site ¹	Wyckoff	<i>x</i>	<i>y</i>	<i>z</i>	U_{eq}	BVS ²
A(1)	4 <i>b</i>	0.5	0	0	0.0244(7)	1.19
A(2)′	4 <i>e</i>	0	0.9889(2)	0.25	0.0365(10)	0.68
M(1)	4 <i>e</i>	0	0.26621(6)	0.25	0.0121(2)	1.89
M(2)	8 <i>f</i>	0.28084(4)	0.65626(4)	0.36949(8)	0.00977(16)	2.46
T(1)	4 <i>e</i>	0	0.71652(3)	0.25	0.00872(10)	5.05
T(2)	8 <i>f</i>	0.23700(3)	0.89104(2)	0.12751(4)	0.00979(9)	5.06
O(1)	8 <i>f</i>	0.45605(18)	0.70881(16)	0.5254(3)	0.0138(4)	2.01
O(2)	8 <i>f</i>	0.10503(19)	0.36634(17)	0.7439(4)	0.0191(5)	2.00
O(3)	8 <i>f</i>	0.33349(18)	0.66891(16)	0.1141(3)	0.0136(4)	2.00
O(4)	8 <i>f</i>	0.11800(19)	0.40465(16)	0.3127(3)	0.0163(4)	2.04
O(5)	8 <i>f</i>	0.22280(18)	0.81846(16)	0.3269(3)	0.0131(4)	1.92
O(6)	8 <i>f</i>	0.3328(2)	0.50558(16)	0.3902(4)	0.0181(5)	1.96

¹ Refined occupancy of the A(1) site is Na 0.788(12) and Ca 0.212(12). For occupancies of the A(2)′ and M sites see Table 6; the T sites are occupied by As⁵⁺. ² Bond-valence parameters were taken from [22]. Bond-valence sums were calculated taking into account cation distribution (see Table 6).

Table 5. Selected interatomic distances (\AA) in the crystal structure of manganobadalovite.

A(1)O ₆ polyhedron	A(1)–O(4)x2	2.366(2)
	A(1)–O(2)x2	2.374(2)
	A(1)–O(4)x2	2.563(2)
	<A(1)–O>	2.434
A(2)′O ₈ polyhedron	A(2)′–O(6)x2	2.471(2)
	A(2)′–O(6)x2	2.565(2)
	A(2)′–O(1)x2	2.900(3)
	A(2)′–O(3)x2	2.980(3)
	<A(2)′–O>	2.729
M(1)O ₆ octahedron	M(1)–O(4)x2	2.226(2)
	M(1)–O(1)x2	2.239(2)
	M(1)–O(3)x2	2.251(2)
	<M(1)–O>	2.239
M(2)O ₆ octahedron	M(2)–O(2)	1.992(2)
	M(2)–O(6)	2.031(2)
	M(2)–O(3)	2.056(2)
	M(2)–O(1)	2.087(2)
	M(2)–O(5)	2.077(2)
	M(2)–O(5)	2.190(2)
<M(2)–O>	2.049	
T(1)O ₄ tetrahedron	T(1)–O(1)x2	1.6865(19)
	T(1)–O(2)x2	1.680(2)
	<T(1)–O>	1.683
T(2)O ₄ tetrahedron	T(2)–O(4)	1.660(2)
	T(2)–O(6)	1.685(2)
	T(2)–O(3)	1.6917(19)
	T(2)–O(5)	1.6940(19)
	<T(2)–O>	1.683

Table 6. Refined site-scattering factors and assignment for cation sites in the structure of manganobadalovite (SC—scattering curve used to refine site occupancy; SOF—refined site-occupancy factor; SSF_{exp} and SSF_{calc} —experimental and calculated site-scattering factors).

Site	SC	SOF	SSF_{exp}	Assigned Site Occupancy	SSF_{calc}
A(2)′	Na	0.88	9.68	$Na_{0.80}Ca_{0.05}$	9.80
M(1)	Mn	0.83	20.75	$Mn^{2+}_{0.55}Ca_{0.18}Mg_{0.15}Na_{0.12}$	20.47
M(2)	Fe	0.82	21.32	$Fe^{3+}_{0.53}Mg_{0.32}Mn_{0.15}$	21.37

4. Discussion

Manganobadalovite belongs to the alluaudite group and adopts the alluaudite structure type, the same as badalovite and all other anhydrous alluaudite-group arsenates. The H-free alluaudite-group arsenates are minerals with the general formula $A(2)′A(1)M(1)M(2)_2(AsO_4)_3$ in which the species-defining *M* and *A* cations are as follows: *M* = Mg, Mn^{2+} , Fe^{3+} , Cu^{2+} , Zn, Ca or Na; *A* = Na, K, Ca, Cu^{2+} or vacancy [15]. The alluaudite-type structure contains zig-zag chains formed by the $[M(2)_2O_{10}]$ dimers connected with each other via distorted $M(1)O_6$ octahedra isolated from each other. $T(1)O_4$ tetrahedra share all vertices with the *M*-centered octahedra, forming the (010) layers, while each $T(2)O_4$ tetrahedron shares three vertices with the *M*-centered octahedra of one layer and the fourth vertex with the octahedron of an adjacent layer, thus linking the layers into a three-dimensional framework. The framework contains channels of two types in which the large cation positions *A*(1), *A*(1)′, *A*(1)″ and *A*(2), *A*(2)′ and *A*(2)″ are located ([15] and references therein).

In the structure of manganobadalovite (Figure 3), both *A*(1) and *A*(2)′ sites are predominantly occupied by Na; the average *A*(1)–O distance is 2.434 Å and that of *A*(2)′–O is 2.729 Å. None of other *A* sites in the channels are filled. The *M*(1) site is occupied by Mn^{2+} with admixtures of Ca, Mg and Na; the average *M*(1)–O distance is 2.239 Å. The *M*(2) site is occupied by Fe^{3+} , Mg and subordinate Mn; the average *M*(2)–O distance is 2.049 Å. Both tetrahedral sites are occupied by As^{5+} with similar average *T*–O distances of 1.683 Å.

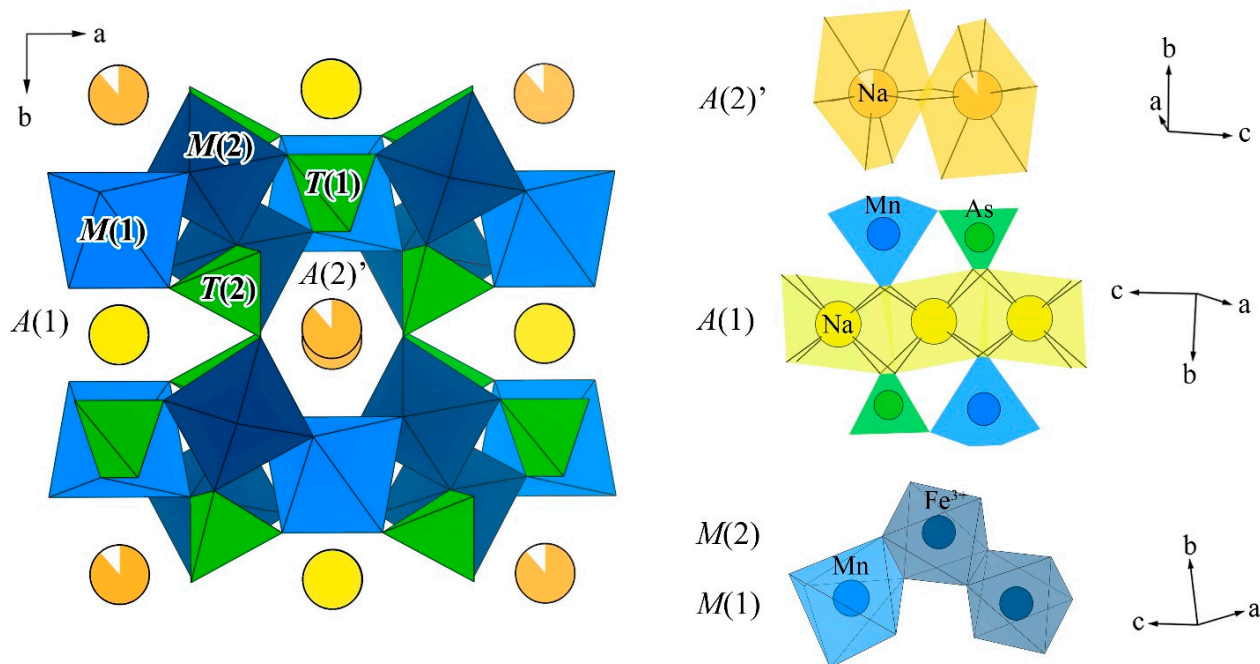


Figure 3. The crystal structure of manganobadalovite in the projection along the *c* axis (left figure) and motifs of AO_8 and MO_6 polyhedra.

The crystal-chemical formula of the studied crystal calculated based on both structure refinement and electron microprobe data is $A^{(1)}(Na_{0.79}Ca_{0.21})_{\Sigma 1.00}A^{(2)'}(Na_{0.80}Ca_{0.05})_{\Sigma 0.85}M^{(1)}(Mn^{2+}_{0.55}Ca_{0.18}Mg_{0.15}Na_{0.12})_{\Sigma 1.00}M^{(2)}(Fe^{3+}_{1.05}Mg_{0.65}Mn_{0.30})_{\Sigma 2.00}(AsO_4)_3$. The simplified crystal-chemical formula can be written as $A^{(1)}Na^{A(2)'}Na^{M(1)}Mn^{2+M(2)}(Mg_{0.5}Fe^{3+}_{0.5})_2(AsO_4)_3$.

Manganobadalovite, ideally $NaNaMn(MgFe^{3+})(AsO_4)_3$, is an analogue of badalovite $NaNaMg(MgFe^{3+})(AsO_4)_3$ and magnesiohatertite $NaNaCa(MgFe^{3+})(AsO_4)_3$ with Mn^{2+} as a prevailing cation in the $M(1)$ site. For this new mineral, we used the rootname “badalovite” but not “hatertite” in agreement with the actual nomenclature of the alluaudite group [15], because both hatertite $NaNaCa(CuFe^{3+})(AsO_4)_3$ and magnesiohatertite contain Ca as a dominant cation in $M(1)$ and differ from one another in species-defining $M(2)$ cations.

Two phosphates of the alluaudite group, varulite $NaNaMn(MnFe^{3+})(PO_4)_3$ and hagen-dorffite $NaNaMn(Fe^{2+}Fe^{3+})(PO_4)_3$ [15], are analogues of manganobadalovite in the ideal composition of the A and $M(1)$ sites.

The Raman spectrum of manganobadalovite is in general similar to the spectra of other anhydrous alluaudite-group arsenates [6,7,9]. To our knowledge, there is no synthetic analogue of manganobadalovite.

Author Contributions: Conceptualization, I.V.P., N.N.K. and D.Y.P.; methodology, I.V.P., N.V.Z., N.N.K. and S.N.B.; fieldworks I.V.P., A.A.A., A.G.T., N.N.K., E.G.S. and E.S.Z.; investigation, N.N.K., I.V.P., D.I.B., N.V.Z., M.F.V., A.A.A., S.N.B. and A.G.T.; writing—original draft preparation, N.N.K. and I.V.P.; writing—N.N.K., I.V.P. and N.V.Z.; visualization, N.N.K.; supervision, I.V.P. and D.Y.P. Author Evgeny G. Sidorov passed away prior to the publication of this manuscript. All authors have read and agreed to the published version of the manuscript.

Funding: This work in part of mineralogical studies, crystal chemical analysis and crystal structure solution was supported by the Russian Science Foundation, grant no. 25-17-00005 (I.V.P., D.Y.P., N.V.Z. and M.F.V.). The powder XRD study was performed at the Center for X-Ray Diffraction Research of the Science Park of St. Petersburg State University within the framework of project 125021702335-5.

Data Availability Statement: The original contributions presented in this study are included in the article. Further inquiries can be directed to the corresponding author.

Acknowledgments: We thank Maria D. Milshina for color photograph of manganobadalovite.

Conflicts of Interest: The authors declare no conflicts of interest.

References

1. Fedotov, S.A.; Markhinin, Y.K. (Eds.) *The Great Tolbachik Fissure Eruption*; Cambridge University Press: New York, NY, USA, 1983; p. 341.
2. Bosi, F.; Hatert, F.; Pasero, M.; Mills, S.J. IMA Commission on New Minerals, Nomenclature and Classification (CNMNC)—Newsletter 86. *Eur. J. Mineral.* **2025**, *37*, 549–553. [[CrossRef](#)]
3. Hålenius, U.; Hatert, F.; Pasero, M.; Mills, S.J. New minerals and nomenclature modifications approved in 2016. *Mineral. Mag.* **2016**, *80*, 1315–1321. [[CrossRef](#)]
4. Bosi, F.; Hatert, F.; Pasero, M.; Mills, S.J. IMA Commission on New Minerals, Nomenclature and Classification (CNMNC)—Newsletter 77. *Eur. J. Mineral.* **2024**, *36*, 165–172. [[CrossRef](#)]
5. Miyawaki, R.; Hatert, F.; Pasero, M.; Mills, S.J. IMA Commission on New Minerals, Nomenclature and Classification (CNMNC)—Newsletter 62. *Eur. J. Mineral.* **2021**, *33*, 479–484. [[CrossRef](#)]
6. Pekov, I.V.; Koshlyakova, N.N.; Belakovskiy, D.I.; Vigasina, M.F.; Zubkova, N.V.; Agakhanov, A.A.; Britvin, S.N.; Sidorov, E.G.; Pushcharovsky, D.Y. New arsenate minerals from the Arsenatnaya fumarole, Tolbachik volcano, Kamchatka, Russia. XVII. Paraberzeliite, $NaCaCaMg_2(AsO_4)_3$, an alluaudite-group member dimorphous with berzeliite. *Mineral. Mag.* **2022**, *86*, 103–111. [[CrossRef](#)]
7. Pekov, I.V.; Koshlyakova, N.N.; Belakovskiy, D.I.; Vigasina, M.F.; Zubkova, N.V.; Agakhanov, A.A.; Britvin, S.N.; Sidorov, E.G.; Pushcharovsky, D.Y. New arsenate minerals from the Arsenatnaya fumarole, Tolbachik volcano, Kamchatka, Russia. XVIII. Khrenovite, $Na_3Fe^{3+}_2(AsO_4)_3$, the member with the highest sodium in the alluaudite supergroup. *Mineral. Mag.* **2022**, *86*, 897–902. [[CrossRef](#)]

8. Pekov, I.V.; Koshlyakova, N.N.; Agakhanov, A.A.; Zubkova, N.V.; Belakovskiy, D.I.; Vigasina, M.F.; Turchkova, A.G.; Sidorov, E.G.; Pushcharovsky, D.Y. New arsenate minerals from the Arsenatnaya fumarole, Tolbachik volcano, Kamchatka, Russia. XV. Calciojohillerite, $\text{NaCaMgMg}_2(\text{AsO}_4)_3$, a member of the alluaudite group. *Mineral. Mag.* **2021**, *85*, 215–223. [[CrossRef](#)]
9. Pekov, I.V.; Koshlyakova, N.N.; Agakhanov, A.A.; Zubkova, N.V.; Belakovskiy, D.I.; Vigasina, M.F.; Turchkova, A.G.; Sidorov, E.G.; Pushcharovsky, D.Y. New arsenate minerals from the Arsenatnaya fumarole, Tolbachik volcano, Kamchatka, Russia. XIV. Badalovite, $\text{NaNaMg}(\text{MgFe}^{3+})(\text{AsO}_4)_3$, a member of the alluaudite group. *Mineral. Mag.* **2020**, *84*, 616–622. [[CrossRef](#)]
10. Pekov, I.V.; Koshlyakova, N.N.; Zubkova, N.V.; Lykova, I.S.; Britvin, S.N.; Yapaskurt, V.O.; Agakhanov, A.A.; Shchipalkina, N.V.; Turchkova, A.G.; Sidorov, E.G. Fumarolic arsenates—A special type of arsenic mineralization. *Eur. J. Mineral.* **2018**, *30*, 305–322. [[CrossRef](#)]
11. Koshlyakova, N.N.; Zubkova, N.V.; Pekov, I.V.; Giester, G.; Sidorov, E.G. Crystal chemistry of johillerite. *Can. Mineral.* **2018**, *56*, 189–201. [[CrossRef](#)]
12. Pekov, I.V.; Zubkova, N.V.; Yapaskurt, V.O.; Belakovskiy, D.I.; Lykova, I.S.; Vigasina, M.F.; Sidorov, E.G.; Pushcharovsky, D.Y. New arsenate minerals from the Arsenatnaya fumarole, Tolbachik volcano, Kamchatka, Russia. I. Yurmarinite, $\text{Na}_7(\text{Fe}^{3+}, \text{Mg}, \text{Cu})_4(\text{AsO}_4)_6$. *Mineral. Mag.* **2014**, *78*, 905–917. [[CrossRef](#)]
13. Shchipalkina, N.V.; Pekov, I.V.; Koshlyakova, N.N.; Britvin, S.N.; Zubkova, N.V.; Varlamov, D.A.; Sidorov, E.G. Unusual silicate mineralization in fumarolic sublimates of the Tolbachik volcano, Kamchatka, Russia—Part 1: Neso-, cyclo-, ino- and phyllosilicates. *Eur. J. Mineral.* **2020**, *32*, 101–119. [[CrossRef](#)]
14. Pekov, I.V.; Agakhanov, A.A.; Zubkova, N.V.; Koshlyakova, N.N.; Shchipalkina, N.V.; Sandalov, F.D.; Yapaskurt, V.O.; Turchkova, A.G.; Sidorov, E.G. Oxidizing-type fumaroles of the Tolbachik volcano, a mineralogical and geochemical unique. *Russ. Geol. Geophys.* **2020**, *61*, 675–688. [[CrossRef](#)]
15. Hatert, F. A new nomenclature scheme for the alluaudite supergroup. *Eur. J. Mineral.* **2019**, *31*, 807–822. [[CrossRef](#)]
16. Britvin, S.N.; Dolivo-Dobrovolsky, D.V.; Krzhizhanovskaya, M.G. Software for processing the X-Ray powder diffraction data obtained from the curved image plate detector of Rigaku RAXIS Rapid II diffractometer. *Zap. Ross. Mineral. Obs.* **2017**, *146*, 104–107. (In Russian)
17. Rigaku Oxford Diffraction. *CrysAlisPro Software System*, version 1.171.39.46; Rigaku Corporation: Oxford, UK, 2018.
18. Sheldrick, G.M. Crystal structure refinement with SHELXL. *Acta Crystallogr.* **2015**, *71*, 3–8.
19. Symonds, R.B.; Reed, M.H. Calculation of multicomponent chemical equilibria in gas-solid-liquid systems; calculation methods, thermo-chemical data, and applications to studies of high-temperature volcanic gases with examples from Mount St. Helens. *Am. J. Sci.* **1993**, *293*, 758–864. [[CrossRef](#)]
20. Nakamoto, K. *Infrared and Raman Spectra of Inorganic and Coordination Compounds*; John Wiley & Sons: New York, NY, USA, 1986.
21. Mandarino, J.A. The Gladstone–Dale compatibility of minerals and its use in selecting mineral species for further study. *Can. Mineral.* **2007**, *45*, 1307–1324. [[CrossRef](#)]
22. Gagné, O.C.; Hawthorne, F.C. Comprehensive derivation of bond-valence parameters for ion pairs involving oxygen. *Struct. Sci.* **2015**, *71*, 562–578. [[CrossRef](#)] [[PubMed](#)]

Disclaimer/Publisher’s Note: The statements, opinions and data contained in all publications are solely those of the individual author(s) and contributor(s) and not of MDPI and/or the editor(s). MDPI and/or the editor(s) disclaim responsibility for any injury to people or property resulting from any ideas, methods, instructions or products referred to in the content.